Research Article: Open Access

VIBGYOR ePress

International Journal of Nanoparticles and Nanotechnology

ISSN: 2631-5084

Production of Ultrafine Ag Nanoparticles by Laser Ablation in Diluted Sodium Borohydride Solution and Their Antibacterial Properties

***Raid Baiee*[1,2*]*, Zhu Liu*[1,2] *and Lin Li*[2]**

[1]*School of Materials, The University of Manchester, UK*

[2]*Laser Processing Research Centre, School of Mechanical, Aerospace and Civil Engineering, The University of Manchester, UK*

Ultra-fine (< 10 nm) nanoparticles are desirable for higher reactivity with the surrounding media due to their higher surface area to volume ratios. They are, however, difficult to produce. The use of laser ablation in liquid could produce high purity nanoparticles in a single process.

Until now, using laser ablation in liquid could only produce Ag nanoparticles with sizes stretching to 20 nm and an average size greater than 7 nm. In this paper, we report a special laser-based method for the production of ultrafine silver nanoparticles with an average size of 5 ± 2.4 nm and maximum nanoparticles up to 10 nm in size by using laser ablation a silver plate immersed in diluted sodium borohydride. A diode pumped Nd:YAG laser emitting at the second harmonic (532 nm) wavelength with a pulse duration of 7 ns was used to generate the Ag nanoparticles. It has been shown that increasing the concentration of sodium borohydride and decreasing the laser fluence lead to a decrease the average and maximum particle sizes of the silver nanoparticles. Stronger antibacterial activity of generated Ag NPs against Gram-negative bacteria - *E. coli* was found compared with nanoparticles generated in deionised water without sodium borohydride.

Keywords

Nanoparticles, Ultrafine, High purity, Ablation, Laser, Ag, Silver, Surfactant

Introduction

Nanoparticles (NPs), i.e., particles with their sizes below 100 nm have attracted much attention in the last few decades because of their unique properties which are different from their bulk materials. An important group of these NPs are the metallic NPs due to their specific applications in many fields including biomedical [1-4], optical [5,6], electronic [7,8] sectors as well as additives to improve the performance of concrete [9,10]. The desired properties of these NPs are strongly depended on their size and shape [11-13]. Therefore, many techniques including physical [14-17], chemical [18,19] and biological [20-22] methods have been developed for the synthesis of nanomaterials. One of the recently development methods is laser ablation of solid targets in liquid [23]. This technique is a single step process based on the ablation of a solid target in liquid and different types of liquid media can serve as a medium providing that they are transparent to the laser beam used. A key challenge in the preparation of metal nanoparticles in solutions is to control the size and shape of the nanoparticles to the desired specification [11,12,24].

Materials in nanoscales have a large surface-to-volume ratio. Therefore, many physical, chemical, and biological characteristics of NPs could be altered by reducing their sizes [25,26]. For instance, the melting point of

***Corresponding author:** *Raid Baiee, School of Materials, The University of Manchester; Laser Processing Research Centre, School of Mechanical, Aerospace and Civil Engineering, Manchester M13 9PL, UK*

Accepted: September 06, 2018: **Published:** September 08, 2018

Citation: Baiee R, Liu Z, Li L (2018) Production of Ultrafine Ag Nanoparticles by Laser Ablation in Diluted Sodium Borohydride Solution and Their Antibacterial Properties. Int J Nanoparticles Nanotech 4:018

the gold is changed from 1064 °C to 900 °C when the size of gold is decreased to 4 nm, then starts to decrease dramatically to about 500 °C for sizes ranging from 1 to 2 nm [27]. Another typical example is that the antibacterial activity of NPs strongly depends on their sizes. The effect of different sizes of Ag NPs on Gram-negative bacteria was studied by Zhong, et al. They found that bacterial growth inhibition was shown to be more effective with Ag NPs with an average diameter less than 10 nm [28].

Chemical reduction is the most commonly used method for the synthesis of metal NPs that have colloidal characteristics with well-controlled sizes. A strong reducing agent such as sodium borohydride was used to produce smaller NPs that are monodispersed. Dong, et al. produced Ag NPs with an average diametre of 4 nm using a chemical reducing method [29]. The disadvantage of the chemical method is that it would need several steps for the high purity NPs production and disposal of the chemicals is needed.

Alternatively, laser ablation of a bulk metal immersed in a liquid can produce colloidal metal NPs by rapid vaporisation and condensation of the target material in a single process step [30]. However, the size, size distribution, shape, composition, and structure of the NPs depend on many parameters including laser fluence, pulse duration, laser wavelength, number of pulses delivered to each target spot and type of liquid surrounding the target [11,12,31]. Because liquid environment parameters affect ablation and cluster formation mechanisms, they can be used to adjust the size and the shape of NPs [11,24,31]. Thus, fundamental studies have been accomplished to improve the laser ablation method for reducing the size and size distribution spread of the colloidal NPs. Many investigations have presented the generation of metal nanoparticles by laser ablation in the presence of an ionic surfactant that serves as a medium to control the size of the nanoparticles. Tajdidzadeh M, et al. showed that particle size of Ag-NPs prepared in ethylene glycol ranged from 10 to 60 nm and an average size about 22 nm, whereas, it ranged from 10 to 80 nm with an average size about 27 nm in deionized water [32]. Bae, et al. produced Ag NPs immersed in various concentrations of NaCl solution and pure water. They demonstrated that the presence of the chloride ions in the liquid medium through laser ablation process could reduce the average size of Ag NPs in 5 mM of NaCl solution to 26 nm with a range of 5 to 50 nm [13]. Oscar, et al. showed that the particle size of Ag NPs depend on the concentration of Cetrimonium bromide (CTAB), where, the particle size of Ag-NPs prepared in 10^{-7} mM of CTAB solution ranged from 5 to 45 nm with an average size 14.5 nm [24]. Ag NPs were also generated in water containing sodium dodecyl sulphate (SDS) by Mafune, et al. They showed that the prepared Ag NPs had average diameters of 16.2, 14.9, and 11.7 in the 0.003, 0.01, and 0.05 M concentrations of SDS solution respectively. In addition, they showed that the average diameter of Ag NPs was reduced to 7.9 nm with the particle sizes up to 22 nm by reducing the laser power [33]. All Ag NPs mentioned above, which were prepared using laser ablation in ionic solutions, have particle size distribution stretching beyond 20 nm as the maximum particle size. Therefore, generating Ag NPs with a smaller maximum size is still a challenge.

In the present work, sodium borohydride was used as a surfactant to generate ultrafine Ag NPs by laser ablation of a Ag solid target in liquid. Sodium borohydride ($NaBH_4$) is a compound commonly served as a strong reducing agent in chemical processes. The nanoparticles will be expected to be kept in suspension by repulsive electrostatic forces between the particles, owing to adsorbed borohydride ions [18,29]. In addition, sodium borohydride is a cheaper material than other ionic surfactants such as SDS, CTAB, and ethylene glycol.

Therefore, in the current study, $NaBH_4$ was used as a surfactant to understand its ability in controlling the size and size distribution of Ag NPs by laser ablation. The obtained Ag NPs were characterized using transmission electron microscopy and examined for antimicrobial activity against *Escherichia coli* (*E. coli*) bacteria and compared with larger sized Ag NPs prepared in deionized water by laser ablation.

Materials and Experimental Procedure

Generation of Ag NPs by laser ablation

Ag NPs were produced by pulsed laser ablation of a silver target in liquid. Briefly, a silver plate (99.99% purity) with a thickness of 2 mm and a surface area of 25 × 25 mm^2 was used as the target material. It was sonicated for 15 minutes in ethanol and deionized water to remove surface impurities. Subsequently, the plate was placed at the bottom of a Pyrex glass vessel filled with freshly prepared sodium borohydride solution ($NaBH_4$: > 96% purity from Sigma-Aldrich) diluted with deionised water. Two parts were performed separately in order to study the effect of different concentrations of $NaBH_4$ and different laser fluences on the average size and size distribution of the produced Ag NPs. The laser fluence in the first part was 2.62 J/cm^2 and the concentrations of $NaBH_4$ were 0, 1 and 2 mM respectively. In the second part, the concentration of $NaBH_4$ was fixed to 2 mM and the Ag plate was irradiated by laser with fluences of 1.83, 4.89, and 7.82 J/cm^2 respectively.

In all the experiments, the liquid was 2 mm above the target surface. The silver plate was irradiated by a second harmonic (532 nm) diode pumped Nd:YAG laser with a pulse duration of 7 ns at a 20 kHz repetition rate. The laser beam was focused on the silver plate with a spot size

of 50 μm in diameter. Raster scanning of the laser beam with an x-y galvanometer was carried out on the target surface over a 5 mm^2 area at a velocity of 250 mm/s with a 0.1 mm scanning line spacing between the two tracks. The laser was irradiated at different fluences and the ablation was performed for 40 minutes in all experiments.

Characterization techniques

The prepared nanoparticle solution was characterized using a UV-Visible double beam spectrophotometer (Analytic Jena, SPECORD 250), zeta potential analyser [Zetasizer Nanoseries (Malvern Instruments)], transmission electron microscopy (TEM,CM 20 Philips) at 200 kV accelerating voltage, and the elemental analysis of the silver nanoparticles (NPs) was performed using an Axis Ultra Hybrid x-ray photoelectron spectrometer (XPS, Kratos) equipped with a monochromated aluminium x-ray source at 1486.6 eV.

The samples of Ag NPs for TEM experiment were prepared by depositing a drop of solution on a carbon-coated 200-mesh copper grid and let to dry completely at room temperature. At least 500 NPs were measured to determine the size distribution. The size of each particle was measured from the corresponding TEM images using Image-J programme. Then, the average size of the particles was calculated by adding the sizes of all particles that measured by Image-J programme and divided by the count of those sizes using excel programme.

Bacterial strains and culture

The separated *E. coli* strain 25922 was cultured in Muller-Hinton broth and incubated at 37 °C for 24 hours with shaking at 225 rpm. After incubation, the optical density (OD) of inoculum suspensions was measured at 600 nm and adjusted from 0.08 to 0.1 (OD of 0.1 corresponding to a concentration of $1.5^{*}10^{8}$ colony-forming units/ml). Then, inoculum suspensions were diluted twice to $1.5^{*}10^{6}$ colony-forming units (CFU/ml) for experimental use.

Micro-dilution method for anti-microbial susceptibility testing

The solution of the antibacterial agent was prepared in a liquid growth medium dispensed in a 96-well microtiter plate. After that, each well was inoculated with bacteria inoculum prepared in the same medium after dilution of standardized bacteria suspension adjusted to 0.5 McFarland scale. After well-mixing, the 96-well microtiter plate was incubated at 37 °C for 24 hours [34].

Determination of MIC

Minimum inhibitory concentration (MIC) is defined as the lowest concentration of the NPs that inhibited bacterial growth after 24 hours of incubation at 37 °C. The MIC of Ag NPs generated by laser ablation method immersed in different concentration of $NaBH_4$, was determined against *E. coli* strain 25922.

Antibacterial activity of Ag NPs was examined using the micro-dilution procedure in Muller-Hinton broth. MIC values were determined using a photometer for microtiter plate (Synergy HTX, Biotek, USA) after inoculation of Ag NPs-containing microtiter plate with 100 μl of *E. coli* bacteria. Therefore, for this investigation, freshly grown bacterial inoculum ($1.5^{*}10^{6}$ CFU/ml) of *E. coli* was incubated in the presence of a range of Ag NPs loadings of 5, 10 and 20 mg/L added in each well to observe the bacterial cell. Total solution volume in each well was kept 200 μl. The concentrations of Ag NPs were determined by weighing the silver target before and after laser ablation using a microbalance scale (Sartorius BL 210S with a resolution of 0.1 mg).

An abiotic (OD blank) control was set with only diluted Ag NPs in media (Muller-Hinton broth) without *E. coli* and a positive control was prepared separately with cells in sterile deionized water and $NaBH_4$ solution which was irradiated by the laser to keep the same environment, both having the same volume (200 μl). They were grown separately in each well (Ag NPs with bacteria, abiotic control, and positive control) at 37 °C for 24 hours with shaking at 225 rpm. Two tests were performed for each concentration of Ag NPs; therefore, two wells containing bacterial suspension with Ag NPs and two wells containing only media (Muller-Hinton broth) with Ag NPs were included in this plate.

Optical densities were measured for 24 hours using a plate reader at 600 nm and recorded for each well every 30 min automatically. Optical densities as a function of time for the control samples and the solutions containing different concentrations of Ag NPs, were measured periodically up to 24 hours.

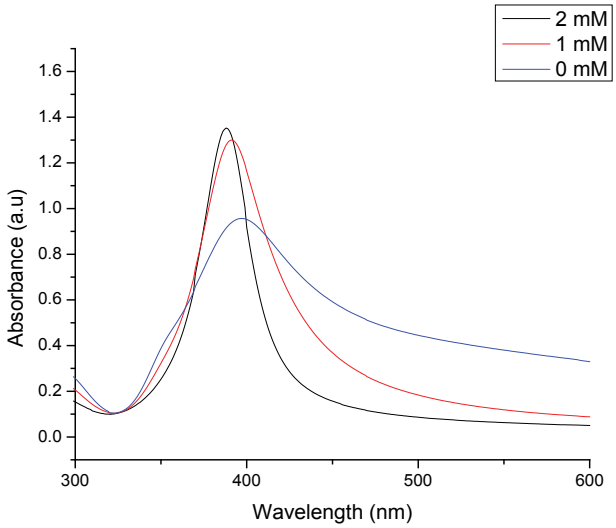

Figure 1: UV-visible absorption spectrum of colloidal silver nanoparticles synthesized in different concentrations of $NaBH_4$ solution at the laser fluence of 2.62 J/cm^2.

Determination of MBC

Minimum bactericidal concentration (MBC) was defined as the lowest concentration that completely kills test bacteria. Therefore, the incubated solution of cells in Ag NPs from each well that showed no growth was further inoculated onto agar plates without any further Ag NPs and incubated at 37 °C for 24 hours to determine the minimum bactericidal concentration (MBC) by streaking the incubated solution on the Mueller Hinton agar plate.

Results and Discussion

Synthesize Ag NPs in diluted $NaBH_4$

Figure 1 shows UV-vis spectra of colloidal solutions obtained by laser ablation of a silver plate in three different concentrations of $NaBH_4$ at a constant laser fluence of 2.62 J/cm^2. From Figure 1 one can observe that the broadest peak is that with pure deionised water without $NaBH_4$. As the concentration of $NaBH_4$ concentration increased, the absorption peak shifted towards shorter wavelengths and became narrower. At the 2 mM $NaBH_4$ concentration, the absorption peak shifted to 388 nm from 397 nm (pure deionised water). Further increase in concentration of sodium borohydride did not show any major change in shifting of absorption peak.

It is well known that the size and size distribution of Ag nanoparticles affect their UV-vis peaks where narrower peaks indicate a narrower size distribution and shorter wavelength indicate smaller NP sizes. These results coincide with the TEM observations of particle sizes shown Figure 2.

Figure 2 depicts typical TEM images and size distributions of Ag nanoparticles prepared in deionised water (0 M of $NaBH_4$) and different concentrations of sodium borohydride and the laser fluence of 2.62 J/cm^2 was fixed for all samples. As clearly seen, the silver nanoparticles prepared in sodium borohydride solutions were more dispersed than those prepared in deionized water. Especially for those prepared in a higher concentration of $NaBH_4$ the particle size was clearly decreased. In addition, Ag NPs generated in deionized water showed an irregular shape with a broader size distribution while Ag NPs generated in $NaBH_4$ were almost spherical with a narrower size distribution. For the aqueous medium with 1 mM of sodium borohydride, the average size was 6.7 ± 3.7 nm, whereas with deionized water it was 28 ± 16.9 nm. With the increase in the concentration of the $NaBH_4$ from 0 to 2 mM, it resulted in Ag nanoparticles of more uniform sizes and a smaller average size as shown in Figure 2. The observations indicated a significant decrease in the average size and maximum size of the nanoparticles with increasing $NaBH_4$ concentration from 0 to 2 mM. The average sizes of nanoparticles were 6.7 ± 3.7 nm and 5.6 ± 2.8 nm for nanoparticles prepared in 1 mM, and 2 mM of $NaBH_4$ respectively. At a concentration higher than 2 mM there was no significant decrease in particle size [35].

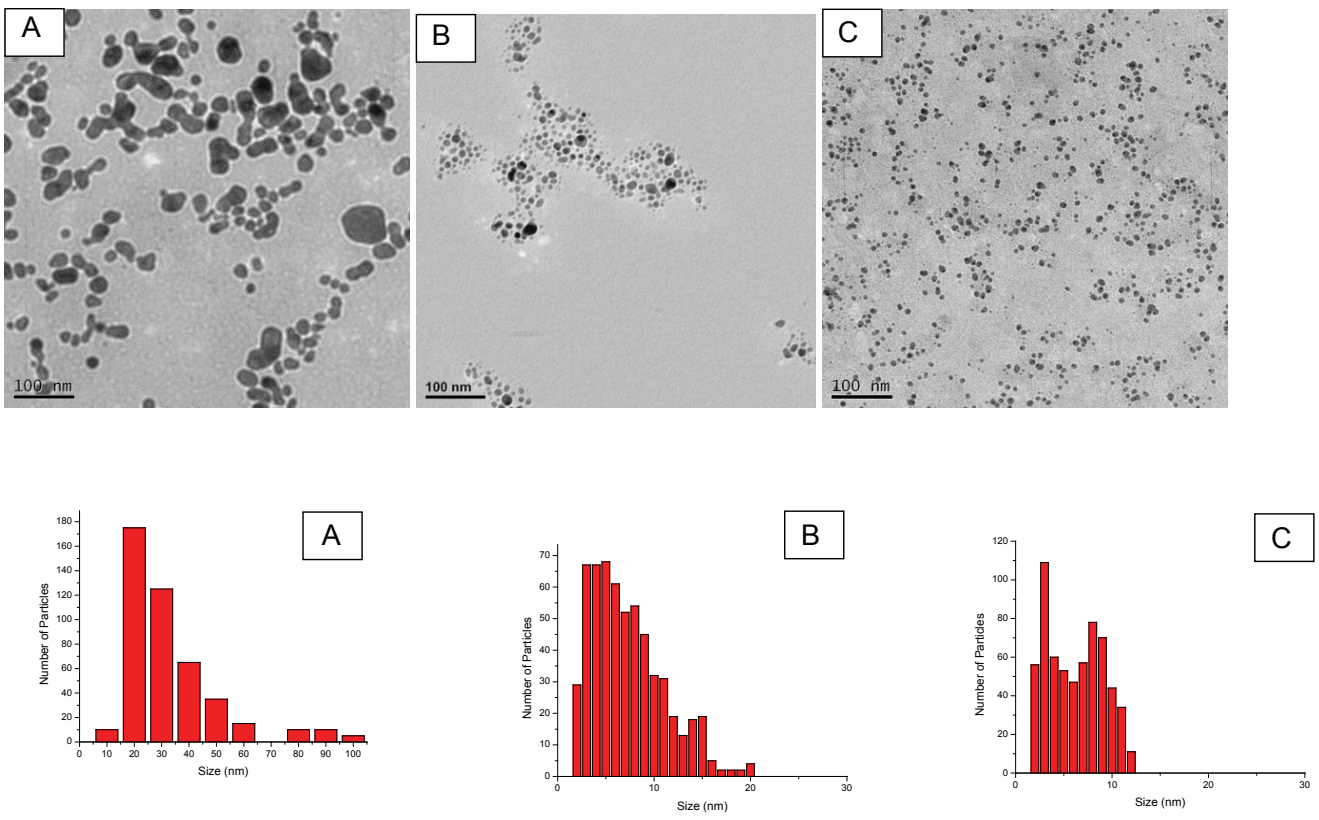

Figure 2: TEM images and size distribution of generated Ag NPs in different concentrations of $NaBH_4$: A) 0 mM; B) 1 mM and C) 2 mM at the laser fluence of 2.62 J/cm^2.

As these figures depict, the laser ablation of an Ag target in different concentrations of $NaBH_4$ could lead to the generation of Ag NPs with different size characteristics. The histograms showed that the different concentrations of $NaBH_4$ could affect the NPs size distribution significantly. For instance, ablation in deionised water resulted in a wider size distribution of Ag NPs ranged from 10 to 100 nm while in the case of ablation in 1 mM of $NaBH_4$; Ag NPs with narrower size distributions from 2 to 20 nm was generated. Moreover, ablation in 2 mM of $NaBH_4$ resulted in even narrower size distribution as the majority of Ag NPs had sizes from 2 to 12 nm and the presence of a large number of smaller size Ag NPs.

The size distribution of the nanoparticles in Figure 2A and Figure 2B revealed a typical Log-Normal distribution which was in agreement with the characteristics of nanoparticles generated by laser ablation in liquid, as reported in Refs. [36,37] that particles grow with supplying silver atoms by diffusion simultaneously to the drift of NPs through a finite growth region. However, the size distribution in Figure 2C showed an additional peak around 8 nm. The presence of the second peak was unlikely to be caused by the increase of $NaBH_4$ concentration for laser ablation, but the collection of the nanoparticles from the solution for the size measurement.

The dynamic formation mechanism of particles in an ionic surfactant- containing solution was explained by Mafun, et al. [38]. Briefly, in the case of ablation with a ns laser, as the laser generated hot plume adiabatically expands, it will be cooled and condensed; therefore, fine particles such as free atoms or clusters collide to each other and nucleate during the ablation. As a result, the embryonic Ag particles are formed by collisional sticking and aggregation in the vapour phase of the plasma plume species [12]. The particles further grow slowly with supplying silver atoms by diffusion; however, when the surfaces of nanoparticles are covered with the ionic surfactant molecules, the growth will be inhibited [38]. In other words, ablation of metals in electrolyte solutions leads to the generation of nanoparticles with smaller sizes because of the formation of electrical double layers (EDL) on the surface of charged nanoparticles, which neutralize any further aggregation [39]. This means that there is a competition between the incorporation of atoms to the nanoparticles growing them and the covering of the existing nanoparticles with surfactant preventing further nanoparticle growth.

In our case, the condensations of the Ag plasma/vapour plume species in the $NaBH_4$ solution resulted in the synthesis of Ag nanoparticles coated with EDL where dissolving $NaBH_4$ in water can release abundance of borohydride ions (BH^-_4) [40].

Therefore, the mechanism of generating smaller Ag NPs by using sodium borohydride would be that $NaBH_4$ creates a strong EDL which restricts the nucleation and growth of NPs.

The first mechanism would be the restriction of the growth of nanoparticles due to the electrical interaction between species, which formed by a direct nucleation in the condense plume, and EDL during the laser ablation. These species would be nucleated and interact with the BH^-_4 to provide nucleation centres for the next incoming silver species [11].

The second mechanism is that Ag atoms clusters were released to the aqueous solution during the laser ablation of target and with the elapsed time. The nucleation occurred as the concentration of Ag atoms reached the critical super saturation which led to the formation of nuclei. By further addition of free Ag atoms in the solution, the nuclei were grown into the nanoscale particles at the same time the BH^-_4 were adsorbed at the particle surface resulting in the highly charged entities which eventually shatter due to charge repulsion [11,33].

The BH^-_4 would create strong negative charged layers around the NPs; therefore, the nanoparticle growth would become restricted during the laser ablation because of electrical interaction between particles and this layer. The growth rate of nanoparticles depends on number of Ag particles formed and the extend of EDL where in the presence of a high concentration of sodium borohydride, the growth rate of the particle is limited and finally halted as the EDL value increases, thereby preventing processes such as nuclei coalescence and atoms from the solvent vicinity. In other words, nanoparticle formation must minimize the particle growth rate relative to the nuclei formation rate in order to obtain small size nanoparticles [41]. As a result, the average size and size distribution would be smaller compared with laser ablation process in water.

The surface charge of the prepared Ag NPs was measured by their zeta-potentials and the measurements were taken immediately after preparation for each sample. The values of zeta potentials were -30.2 mV, -36.5 mV, and -47.3 mV for samples prepared in 0, 1 and 2 mM $NaBH_4$ respectively. It was shown that increasing the $NaBH_4$ concentration lead to an increase of the value of zeta potential which is a good indicator for increasing the repulsion power of Ag NPs against the agglomeration. i.e., increasing the concentration of $NaBH_4$ leads to decreasing the agglomeration of Ag NPs because of the existence of a strong negative charged layer on the surface of Ag NPs. As a result, average size and size distribution of generated Ag NPs depend on the electrolyte concentration of liquid environment.

Preparation Ag NPs at different laser fluences

Another factor which can effect the average size and

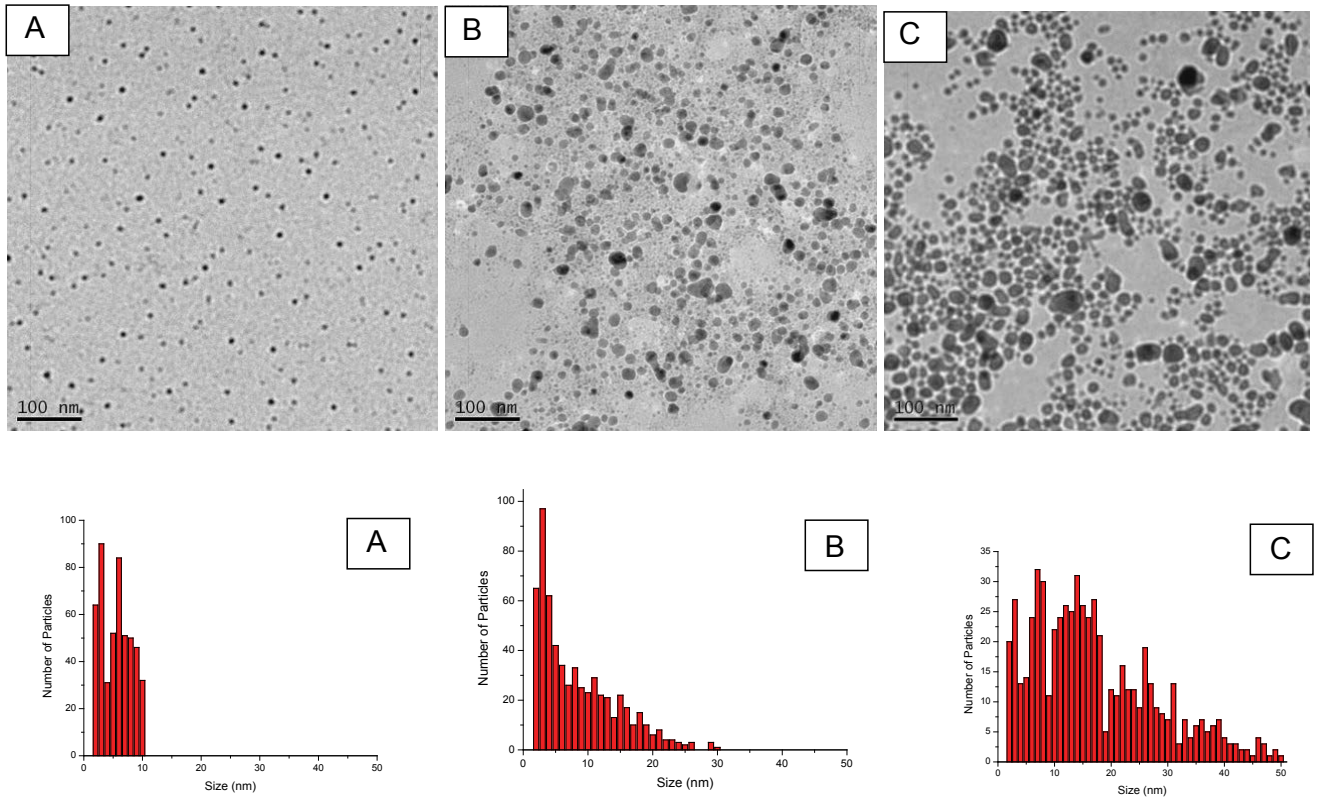

Figure 3: TEM images and size distributions of the Ag NPs produced by laser ablation in a 2 mM $NaBH_4$ aqueous solution at the various laser fluence. The laser fluence for A, B, and C are 1.83, 4.89, and 7.82 J/cm^2 respectively.

size distribution of Ag NPs is the laser fluence. The generation of Ag NPs at different laser fluences in the $NaBH_4$ environment was investigated. The results showed that the average size and size distribution of generated Ag NPs at various laser fluences were different. As the laser fluence decreased, the average size of Ag NPs was reduced and size distribution became narrower. Figure 3 shows Ag NPs prepared at different fluences in 2 mM of $NaBH_4$. The average size of Ag NPs was 5 ± 2.4, 7.9 ± 5.9, and 16.6 ± 10.9 nm for runs with the laser fluences of 1.83, 4.89, and 7.82 J/cm^2 respectively. In addition, the histogram in Figure 3 indicates a large change in the particle size distribution of the prepared Ag NPs with the increase in laser energy. The synthesized Ag NPs had size distributions between 2 to 10 nm, 2 to 30 nm, and 2 to 50 nm for runs with the laser fluences of 1.83, 4.89 and 7.82 J/cm^2 respectively.

Laser fluence directly affected the size of prepared Ag NPs by two mechanisms.

Firstly, at a higher fluence, NPs are not only formed by nucleation and growth of particles in a dense plasma cloud during laser ablation but are also formed by the ejection of metal droplets from the target; therefore, increasing the laser fluence leads to an increase in the agglomeration probability because of increment of the melting depth of the target surface and amount of target material simultaneously appeared in liquid [42,43].

The second mechanism is that thermodynamic properties of the cavitation bubbles and the produced plasma are directly affected by the laser fluence; therefore, increasing laser fluence allows the plasma plume to reach a higher temperature and pressure which leads to longer duration of the cavitation bubbles and cooling. In other words, when the plasma plume reaches a higher temperature and pressure by increasing the laser fluence, the life of cavitation bubbles will be longer before they collapse which would result in the formation of larger size particles by coalescence [41].

An important factor that influences the size properties of Ag NPs is the dynamic formation mechanism as explained in a model by Mafuné, et al. [33]. According to this model, size properties decreases with a decrease in the laser power and increase with an increase in the surfactant concentration. This can be demonstrated according to their model in term of rapid formation of an embryonic Ag NPs and a consecutive particle growth in competition with termination of the growth because of adsorbing of BH^-_4 on the particle. This is because a dense cloud of silver atoms is built over the laser spot of the metal plate, immediately after the laser ablation. Therefore, if the inter atomic interaction is much stronger than the interaction between a silver atom and BH^-_4 which is released from $NaBH_4$, silver atoms are aggregated as much as silver atoms are supplied.

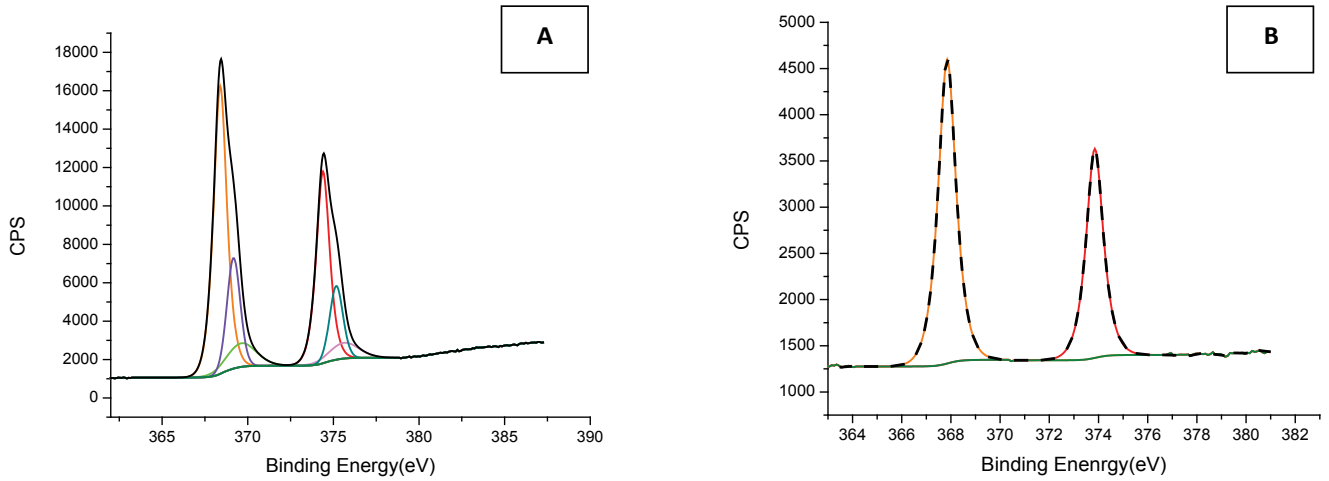

Figure 4: XPS spectra of Ag NPs produced by laser ablation method in A) Deionised water with the laser fluence of 2.62 J/cm^2 and B) 2 mM $NaBH_4$ solution with the laser fluence of 1.83 J/cm^2.

Finally, the smallest and the most homogeneous Ag NPs were synthesized at lower laser fluence and higher concentration of $NaBH_4$.

X-ray photoelectron spectroscopy (XPS) analysis of Ag NPs

The elemental analysis of the silver nanoparticles was performed using the x-ray photoelectron spectroscopy (XPS) analysis. The spectra were measured with analyser pass energy of 20 eV and at an instrument vacuum pressure of $< 3 \times 10^{-8}$ mbar. Figure 4A depicts the XPS analysis of Ag compound nanoparticles prepared in deionised water. The results showed that the Ag 3d spectrum in Figure 4A consists of two pairs of doublet peaks of Ag 3d3/2 and Ag 3d5/2. Two big peaks that located at 368.3 and 374.3 eV and the two small peaks located at 369.1 and 375.1 eV are found to be attributed to the silver metal (Ag^o) [44,45]. In addition, other two small peaks that located at 369.6 and 375.6 are assigned to silver in ionic state (Ag^{2+}) [46].

Figure 4B shows the Ag 3d XPS spectra of Ag NPs generated by laser ablation in $NaBH_4$, and two peaks located at approximately 373.8 and 367.8 eV can be observed. These peaks are attributed to metallic silver [47].

The XPS analysis of the NPs produced in deionized water reveals the presence of metallic silver (Ag^o) and ionic silver (Ag^{2+}) whilst the NPs prepared in the $NaBH_4$ solution shows the presence of metallic Ag only. The formation of metallic Ag only in the $NaBH_4$ solution could be attributed to the reduction of the Ag ions by $NaBH_4$. It is known that $NaBH_4$ is a strong reducing agent; therefore, metallic Ag nanoparticles are more likely to be produced in a reducing agent. This was also reported in reference [29] regarding formation of metallic Ag nanoparticles in $NaBH_4$ solution using a chemical method.

Antibacterial activity

The antibacterial activity of Ag NPs prepared by laser ablation in 0 mM and 2 mM of $NaBH_4$ solution against Gram negative bacteria was examined using the micro-dilution method to determine the MIC.

Ag NPs size effect on MIC: Figure 5 depicts bacterial growth curves at different Ag NPs concentrations (5-20 mg/L). A higher value of optical density (OD) represents growth of bacteria, indicating lower antibacterial activity where the optical density is related to the bacteria cell survival. Therefore, Figure 5B shows that the growth of bacteria was the same as the growth of bacteria treated with water (control), suggesting that $NaBH_4$ solution had no bactericidal activity.

In addition, it can be clearly seen that the growth inhibition rate of the tested bacteria depends strongly on the size of Ag NPs where the MIC was 20 mg/L for the sample prepared in deionized water, it was 10 mg/L for the sample synthesized in $NaBH_4$. In addition, it should be noted that the delay growth rate of bacteria at 5 mg/L of Ag NPs synthesized in $NaBH_4$ was higher than Ag NPs generated in deionized water indicated by a comparison of OD value in Figure 5A and Figure 5B. This means that the Ag NPs generated in $NaBH_4$ affected the antibacterial activity of Ag NPs toward *E. coli* to different extents. Specifically, the antibacterial activity of Ag NPs was evidently enhanced using Ag NPs generated in $NaBH_4$ containing solution. Consistent with a previous study, smaller size of Ag NPs showed a higher bactericidal effect than bigger sizes of Ag NPs at the same dose of 10 and 5 mg/L where we can see from Figure 5 that the OD decreased with decreasing the size of Ag NPs, indicating complete death of bacteria at 10 mg/L and there was no bacteria growth within 12 hours at 5 mg/L in the suspensions. In other words, the *E. coli* growth curves recorded in the presence of 10 and 5 mg/L of Ag NPs revealed that the strongest and most efficient hindering of bacteria growth with Ag NPs of 5 ± 2.4 nm in average size where it is ob-

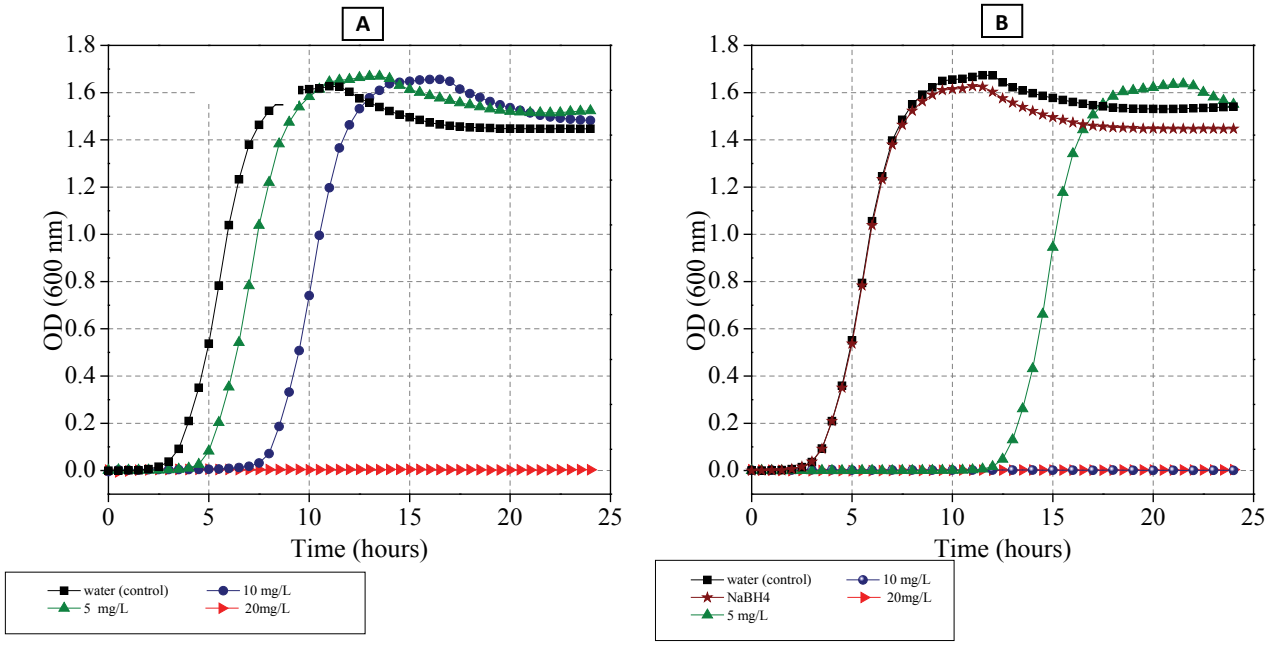

Figure 5: Growth kinetics curve of *E. coli* in the presence of different concentrations of Ag NPs prepared in A) Water and B) $NaBH_4$ solutions respectively.

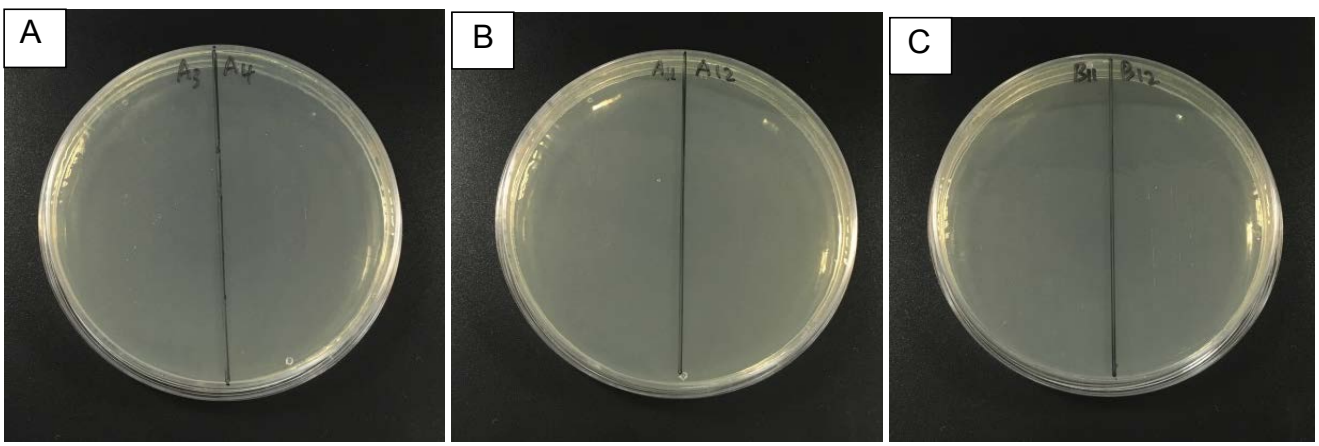

Figure 6: Petri dishes streak after determination of MIC of Ag NPs which were prepared in A) Water; B) and C) $NaBH_4$ respectively and incubated for 24 hours to determine the MBC. The photograph depicts Muller-Hinton broth plates containing the incubated solution of 96 well cells in Ag NPs from each well containing different concentration of Ag NPs: A) 20 mg/L; B) 20 mg/L and C) 10 mg/L respectively.

served from Figure 5 that a 5 mg/L concentration of Ag NPs of 5 ± 2.4 nm delayed the bacterial growth up to 12 hours while Ag NPs of 28 ± 16.9 nm delayed the growth of bacteria up to 4 hours.

This means that the Ag NPs with 5 ± 2.4 nm of mean size strongly influenced the growth of *E. coli* because smaller NPs (< 10 nm) could easily penetrate inside the bacteria and reach its nuclear content [48,49] and smaller size of Ag NPs have increasing of the number of atoms at the surface in comparison to the numbers of atoms in the centre of crystal; as a result, larger surface areas come in contact with the bacteria which results in the higher percentage of interaction with bacteria [28].

MBC of Ag NPs: Although the MIC results showed that 20 mg/L of Ag NPs of 28 ± 16.9 nm and 20 mg/L and 10 mg/L of Ag NPs of 5 ± 2.4 nm presented zero OD, *E. coli* cells could grow back after more than 24 hours of incubation. Therefore, the MBC was used to determine the completeness of killing bacteria. Figure 6 depicts the MBC of Ag NPs. We can see that all the Ag NPs samples completely inhibited the bacteria, i.e. they completely killed the bacteria at the same concentration. This suggests that 28 ± 16.9 nm Ag NPs and 5 ± 2.4 Ag NPs completely inhibited the growth of *E. coli* and killed them at the concentration of 20 and 10 mg/L respectively.

Conclusion

Ultrafine Ag NPs were synthesized by pulsed laser ablation of silver plate in diluted sodium borohydride solu-

tion. The NP sizes ranging from 2 to 10 nm was achieved as a direct result of the addition of sodium borohydride where laser ablation in $NaBH_4$ solution significantly reduced the average size of Ag NPs (5 ± 2.4 nm) compared with that the average size of 28 ± 16.9 nm in deionised water. Furthermore, laser generated Ag NPs in $NaBH_4$ solution showed higher antibacterial activity than Ag NPs obtained by laser ablation in water.

Acknowledgement

The authors would like to thank the Iraqi Ministry of Higher Education and Scientific Research (MOHESR), University of Babylon for sponsoring Mr. R. Baiee's PhD scholarship. The authors also want to thank Irina Barbolina of LIG Biowise Ltd for her biological assistance in bactericidal testing procedures and methods. We also thank B. F. Spencer for performing the XPS analysis.

References

1. Mirzajani F, Ghassempour A, Aliahmadi A, AliEsmaeili M (2011) Antibacterial effect of silver nanoparticles on Staphylococcus aureus. Research in Microbiology 162: 542-549.
2. Rana S, Kalaichelvan P (2011) Antibacterial activities of metal nanoparticles. Advanced Biotech 11: 21-23.
3. Anna Chmielowiec-Korzeniowska, Łukasz Krzosek, Leszek Tymczyna, Magdalena Pyrz, Agata Drabik (2013) Bactericidal, fungicidal and virucidal properties of nanosilver. Mode of action and potential application. A review. 31: 1-11.
4. Díaz-Visurraga J, Gutiérrez C, Von Plessing C, García A (2011) Metal nanostructures as antibacterial agents. In: A Méndez-Vilas, Science against microbial pathogens: Communicating current research and technological advances. Formatex 210-218.
5. Smitha SL, Nissamudeen KM, Philip D, Gopchandrana KG (2008) Studies on surface plasmon resonance and photoluminescence of silver nanoparticles. Spectrochimica Acta Part A: Molecular and Biomolecular Spectroscopy 71: 186-190.
6. Giorgetti E, Giusti A, Arias E, Moggio I, Ledezma A, et al. (2009) In Situ production of polymer-capped silver nanoparticles for optical biosensing. Macromol Sym 283-284: 167-173.
7. Le Guével X, Freddy Y Wang, Ondrej Stranik, Robert Nooney, Vladimir Gubala, et al. (2009) Synthesis, stabilization, and functionalization of silver nanoplates for biosensor applications. The Journal of Physical Chemistry C 113: 16380-16386.
8. Zhu S, C Du, Y Fu (2009) Fabrication and characterization of rhombic silver nanoparticles for biosensing. Optical Materials 31: 769-774.
9. Reches Y (2018) Nanoparticles as concrete additives: Review and perspectives. Construction and Building Materials 175: 483-495.
10. Sanchez F, Sobolev K (2010) Nanotechnology in concrete - A review. Construction and Building Materials 24: 2060-2071.
11. Tilaki R, Mahdavi S (2007) The effect of liquid environment on size and aggregation of gold nanoparticles prepared by pulsed laser ablation. Journal of Nanoparticle Research 9: 853-860.
12. Semaltianos N (2010) Nanoparticles by laser ablation. Critical Reviews in Solid State and Materials Sciences 35: 105-124.
13. Bae CH, Nam SH, Park SM (2002) Formation of silver nanoparticles by laser ablation of a silver target in NaCl solution. Applied Surface Science 197-198: 628-634.
14. Tsuji T, Iryo k, Watanabe N, Tsujiab M (2002) Preparation of silver nanoparticles by laser ablation in solution: influence of laser wavelength on particle size. Applied Surface Science 202: 80-85.
15. Omurzak E, Mashimo T, Sulaimankulova S, Takebe S, Chen L, et al. (2011) Wurtzite-type ZnS nanoparticles by pulsed electric discharge. Nanotechnology 22: 1-7.
16. Pattabi RM, Sridhar KR, Gopakumar S, Vinayachandra B, Pattabi M (2010) Antibacterial potential of silver nanoparticles synthesised by electron beam irradiation. International Journal of Nanoparticles 3: 53-64.
17. Takele H, Jebril S, Strunskus T, ZaporojchenkoV, Adelung R, et al. (2008) Tuning of electrical and structural properties of metal-polymer nanocomposite films prepared by co-evaporation technique. Applied Physics A 92: 345-350.
18. Mulfinger L, Solomon SD, Bahadory M, Jeyarajasingam AV, Rutkowsky SA, et al. (2007) Synthesis and study of silver nanoparticles. J Chem Educ 84: 322-325.
19. Jeong Y, DW Lim, J Choi (2014) Assessment of size-dependent antimicrobial and cytotoxic properties of silver nanoparticles. Advances in Materials Science and Engineering 2014: 1-6.
20. Philip D (2010) Green synthesis of gold and silver nanoparticles using Hibiscus rosa sinensis. Physica E: Low-Dimensional Systems and Nanostructures 42: 1417-1424.
21. Vilchis-Nestor AR, Mendieta VS, Camacho-López MA, Gómez-Espinosa RM, Camacho-Lópezb MA, et al. (2008) Solventless synthesis and optical properties of Au and Ag nanoparticles using Camellia sinensis extract. Materials Letters 62: 3103-3105.
22. Iravani S (2014) Bacteria in nanoparticle synthesis: Current status and future prospects. International Scholarly Research Notices 2014: 1-18.
23. Neddersen J, Chumanov G, Cotton TM (1993) Laser ablation of metals: A new method for preparing SERS active colloids. Applied Spectroscopy 47: 1959-1964.
24. Olea-Mejía O, Pote-Orozco H, Camacho-López MA, Olea-Cardoso O, López-Castañares R, et al. (2013) Silver nanoparticles obtained by laser ablation using different stabilizers. Japanese Journal of Applied Physics 52: 1-6.
25. Abideen SU (2012) Chemiluminescent reactions catalyzed by nanoparticles of gold, silver, and gold/silver alloys. Thesis Department of Chemistry, Eastern Michigan University.
26. Takeshima T, Tada Y, Sakaguchi N, Watari F, Fugetsu B (2015) DNA/Ag nanoparticles as antibacterial agents against gram-negative bacteria. Nanomaterials 5: 284-297.
27. Klabunde KJ, Richards R (2001) Nanoscale materials in chemistry. John Wiley & Sons, Inc.
28. Lu Z, Rong K, Li J, Yang H, Chen R (2013) Size-dependent antibacterial activities of silver nanoparticles against oral

anaerobic pathogenic bacteria. J Mater Sci Mater Med 24: 1465-1471.

29. Van Dong P, Ha CH, Kasbohm J (2012) Chemical synthesis and antibacterial activity of novel-shaped silver nanoparticles. International Nano Letters 2: 1-9.

30. Besner S (2008) Ultrafast laser based “green” synthesis of non-toxic nanoparticles in aqueous solutions. Applied Physics A 93: 955-959.

31. Khilkala WM, Al-Dahash GA, Wahid SNA (2014) Preparation and characterization of Cu nanoparticles by laser ablation in NaOH aqueous solution. International Journal of Current Engineering and Technology 4: 2577-2579.

32. Tajdidzadeh M, Azmi BZ, Yunus WM, Talib ZA, Sadrolhosseini AR, et al. (2014) Synthesis of silver nanoparticles dispersed in various aqueous media using laser ablation. Scientific World Journal 2014: 324921.

33. Mafuné F, Kohno JY, Takeda Y, Kondow T (2000) Formation and size control of silver nanoparticles by laser ablation in aqueous solution. The Journal of Physical Chemistry B 104: 9111-9117.

34. Balouiri M, Sadiki M, Ibnsouda SK (2016) Methods for in vitro evaluating antimicrobial activity: A review. Journal of Pharmaceutical Analysis 6: 71-79.

35. Zamiri R, Azmi BZ, Sadrolhosseini AR, Ahangar HA, Zaidan AW, et al. (2011) Preparation of silver nanoparticles in virgin coconut oil using laser ablation. International Journal of Nanomedicine 6: 71-75.

36. Krstulović N, Salamon K, Budimlija O, Kovač J, Dasović J, et al. (2018) Parameters optimization for synthesis of Al-doped ZnO nanoparticles by laser ablation in water. Applied Surface Science 440: 916-925.

37. Amendola V, Meneghetti M (2013) What controls the composition and the structure of nanomaterials generated by laser ablation in liquid solution? Phys Chem Chem Phys 15: 3027-3046.

38. Mafuné F, Kohno JY, Takeda Y, Kondow T (2000) Structure and stability of silver nanoparticles in aqueous solution produced by laser ablation. The Journal of Physical Chemistry B 104: 8333-8337.

39. Šišková K, Vlčková B, Turpin PY, Fayet C (2008) Ion-specific effects on laser ablation of silver in aqueous electrolyte solutions. The Journal of Physical Chemistry C 112: 4435-4443.

40. Sarioğlan Ş (2013) Recovery of palladium from spent activated carbon-supported palladium catalysts. Platinum Metals Review 57: 289-296.

41. Mahdieh MH, Fattahi B (2015) Size properties of colloidal nanoparticles produced by nanosecond pulsed laser ablation and studying the effects of liquid medium and laser fluence. Applied Surface Science 329: 47-57.

42. Nichols WT, Sasaki T, Koshizaki N (2006) Laser ablation of a platinum target in water. III. Laser-induced reactions. Journal of Applied Physics 100: 1-6.

43. Tyurnina AE, Shur VY, Kozinb RV, Kuznetsov Dk, Mingaliev EA (2013) Synthesis of stable silver colloids by laser ablation in water. Proc SPIE 9065.

44. Hu Y, Zhang AQ, Li HJ, Qian DJ, Chen M (2016) Synthesis, study, and discrete dipole approximation simulation of Ag-Au bimetallic nanostructures. Nanoscale Research Letters 11: 209.

45. Fu S, He Y, Wu Q, Wu Y, Wu T (2016) Visible-light responsive plasmonic Ag_2O/Ag/g-C_3N_4 nanosheets with enhanced photocatalytic degradation of Rhodamine B. Journal of Materials Research 31: 2252-2260.

46. Miller H, Bevilacqua M, Filippi J, Lavacchi A, Marchionni A, et al. (2013) Nanostructured Fe-Ag electrocatalysts for the oxygen reduction reaction in alkaline media. Journal of Materials Chemistry A 1: 13337-13347.

47. Chook SW, Chia CH, Zakaria S, Ayob MK, Chee KL, et al. (2012) Antibacterial performance of Ag nanoparticles and AgGO nanocomposites prepared via rapid microwave-assisted synthesis method. Nanoscale Research Letters 7: 1-7.

48. Lok CN, Ho CM, Chen R, He QY, Yu WY, et al. (2006) Proteomic analysis of the mode of antibacterial action of silver nanoparticles. Journal of Proteome Research 5: 916-924.

49. Morones JR, Elechiguerra JL, Camacho A, Holt K, Kouri JB, et al. (2005) The bactericidal effect of silver nanoparticles. Nanotechnology 16: 2346-2353.